Journal of Sound and Vibration 379 (2016) 135–149

Contents lists available at ScienceDirect

Journal of Sound and Vibration

journal homepage: www.elsevier.com/locate/jsvi

The influence of phase-locking on internal resonance from a nonlinear normal mode perspective

T.L. Hill [a,*], S.A. Neild [a], A. Cammarano [b], D.J. Wagg [c]

[a] Department of Mechanical Engineering, University of Bristol, Bristol BS8 1TR, UK
[b] School of Engineering, University of Glasgow, Glasgow G12 8QQ, UK
[c] Department of Mechanical Engineering, University of Sheffield, Sheffield S1 3JD, UK

ARTICLE INFO

Article history:
Received 18 December 2015
Received in revised form
24 March 2016
Accepted 16 May 2016
Handling Editor: W. Lacarbonara
Available online 6 June 2016

Keywords:
Internal resonance
Nonlinear normal modes
Backbone curves
Nonlinear dynamics
Cable dynamics

ABSTRACT

When a nonlinear system is expressed in terms of the modes of the equivalent linear system, the nonlinearity often leads to modal coupling terms between the linear modes. In this paper it is shown that, for a system to exhibit an internal resonance between modes, a particular type of nonlinear coupling term is required. Such terms impose a phase condition between linear modes, and hence are denoted *phase-locking* terms. The effect of additional modes that are not coupled via phase-locking terms is then investigated by considering the backbone curves of the system. Using the example of a two-mode model of a taut horizontal cable, the backbone curves are derived for both the case where phase-locked coupling terms exist, and where there are no phase-locked coupling terms. Following this, an analytical method for determining stability is used to show that phase-locking terms are required for internal resonance to occur. Finally, the effect of non-phase-locked modes is investigated and it is shown that they lead to a *stiffening* of the system. Using the cable example, a physical interpretation of this is provided.

1. Introduction

Weakly nonlinear systems typically have an underlying linear structure and the underlying linear modes are often used to describe the fundamental components of the system. In this paper we investigate the coupling terms that are present in nonlinear systems when projected onto these linear modes. Specifically, we show how phase-locking conditions in these terms influence the internally resonant dynamic behaviour. Such phenomena are often observed in forced, lightly damped, and weakly nonlinear systems with multiple degrees-of-freedom, which represent a variety of physical applications, see for example [1–4]. Here, internal resonance is defined as the triggering of a dynamic response of a linear mode of the system that is not subjected to direct external excitation. Many previous authors have considered problems of this type, see for example [3,4] and references therein.

In this work we will use the normal form technique proposed by [5] for multi-degree-of-freedom forced, damped, weakly nonlinear systems. This approach leads naturally to the analysis of backbone curves, which define the dynamic behaviour of periodic motions in the unforced and undamped equivalent system, in the amplitude vs frequency plane. These are equivalent to the loci of the nonlinear normal modes (NNMs), represented in the amplitude vs frequency projection.

* Corresponding author.
E-mail address: tom.hill@bristol.ac.uk (T.L. Hill).

http://dx.doi.org/10.1016/j.jsv.2016.05.028

Many authors have considered the NNMs of, for example, a two-degree-of-freedom spring–mass system [6–8]. Lewandowski [9] pointed out that bifurcations can occur in the backbone curves of this type, and the same author went on to analyse beam, membrane and plate examples [10]. More recently, the current authors have used backbone curves to study internal resonance phenomena in systems of coupled nonlinear oscillators [11–14]. In particular, bifurcations of backbone curves were used to indicate where an internal resonance may by triggered, however additional solution branches have also been observed that do not trigger internal resonances. As internal resonance is defined here as a behaviour seen in systems subject to external excitation, and as the backbone curves describe the unforced and undamped responses, it should be noted that the backbone curves themselves do not exhibit internal resonance. However, backbone curves do uncover modal interactions which may lead to internal resonances when external forcing and damping are introduced.

Here, the phenomenon of phase-locking between modes during internal resonance is considered in detail. Much of this discussion is motivated by the example of a taut cable, introduced in Section 2. Expressions for the backbone curves of the cable are developed in Section 3 by considering the interactions between pairs of linear modes. This analysis reveals that, depending on the pairs of modes that are considered, the backbone curves are either phase-locked or phase-unlocked.

One significant feature of phase-locking is revealed in Section 4, where it is shown that phase-locked terms are required for internal resonance. This is demonstrated using an analytical stability analysis, which considers the stability of the zero-amplitude solution of an unforced linear mode of a general weakly nonlinear system. This general analysis is applied to the cable example, demonstrating the physical significance of this observation. Lastly, in Section 5, the cable example is used to investigate the influence of additional, phase-unlocked, modes on the dynamic behaviour of an internally resonant pair of modes. It is shown that, although this type of mode cannot lead to additional internal resonances, they can impose a stiffening effect on the system, altering the response of the phase-locked pair. For the cable, this effect can be explained physically as an increase in the axial tension in the cable, due to the presence of additional modal oscillations.

2. Resonant equations of motion

Weakly nonlinear, multi-degree-of-freedom systems are often expressed in terms of the modal coordinates for the linearised version of the system, as the linear terms will then be decoupled. However, decoupling of the nonlinear terms is typically not achieved via a linear modal transform, and hence the modes will not, in general, match the NNMs of the nonlinear system. Note that here we use the term *modes* to refer to the modes of the linearised system. A multimodal nonlinear system may be written in modal coordinates, $\mathbf{q}$, as

$$\ddot{\mathbf{q}}+\Gamma\dot{\mathbf{q}}+\Lambda\mathbf{q}+\mathbf{N}(\mathbf{q})=\mathbf{f}. \tag{1}$$

Assuming linear modal damping, the kth diagonal elements in diagonal matrices Γ and Λ are $2\zeta_k\omega_{nk}$ and ω_{nk}^2 respectively and the vector $\mathbf{N}$ contains the nonlinear stiffness terms, and $\mathbf{f}$ represents the external excitation vector in modal coordinates. Here, ζ_k and ω_{nk} are used to denote the linear damping ratio and linear natural frequency of the kth mode respectively.

To analyse weakly nonlinear systems it is helpful to transform the equations of motion into a new set of coordinates, $\mathbf{u}$, which describe only the resonant components of the response. The dynamic equation in $\mathbf{u}$ is termed the *resonant* equation of motion. This can then be used to find steady-state solutions, in terms of modal amplitudes, via an exact harmonic balance using trial solutions of the form

$$u_k=U_k\cos\left(\omega_{rk}t-\phi_k\right)=\frac{U_k}{2}\mathrm{e}^{\mathbf{j}(\omega_{rk}t-\phi_k)}+\frac{U_k}{2}\mathrm{e}^{-\mathbf{j}(\omega_{rk}t-\phi_k)}=u_{pk}+u_{mk}, \tag{2}$$

where ω_{rk} is the response frequency of the kth mode and subscripts p and m indicate positive and negative (minus) complex exponential terms respectively. The introduction of ω_{rk} allows for the detuning of the kth mode from the linear natural frequency, ω_{nk}. For a resonant response, this response frequency is typically selected such that it is close to the linear natural frequency of the mode in question, $\omega_{rk}\approx\omega_{nk}$. Note, however, that response frequencies that are not close to the linear natural frequencies may also be selected, as the assumption that this detuning is small is not a requirement of the technique. Normal form analysis allows us to find the periodic responses of a system, as is assumed when computing NNMs, or the steady-state response to a sinusoidal forcing. Taking the period to be $T=2\pi/\Omega$, the response frequency of the kth mode, ω_{rk}, is an integer multiple of Ω. Likewise, if the system is forced at a single frequency, the forcing frequency is an integer multiple of Ω.

If forcing is near-resonant, i.e. the frequency of the forcing acting on any mode is close to the natural frequency of that mode, or if there is no forcing, then the resonant equation of motion is found by applying a nonlinear near-identity transform to Eq. (1) to give

$$\ddot{\mathbf{q}}+\Gamma\dot{\mathbf{q}}+\Lambda\mathbf{q}+\mathbf{N}(\mathbf{q})=\mathbf{f}\xrightarrow{\mathbf{q}=\mathbf{u}+\mathbf{h}(\mathbf{u})}\ddot{\mathbf{u}}+\Gamma\dot{\mathbf{u}}+\Lambda\mathbf{u}+\mathbf{N}_u(\mathbf{u})=\mathbf{f}, \tag{3}$$

where $\mathbf{h}$ is a vector of harmonic components. In the formulation shown in Eq. (3), it is assumed that the forcing and damping terms are resonant, and so are retained in the equation for $\mathbf{u}$. For further discussion of how non-resonant terms are handled see [5,15]. Additionally, details of how the harmonics $\mathbf{h}$ and the transformed nonlinear terms $\mathbf{N}_u$ are found are given in the Appendix.

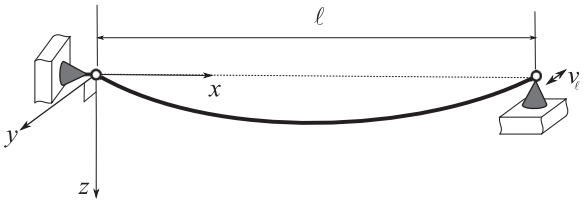

Fig. 1. Schematic diagram showing a taut cable excited horizontally.

2.1. Resonant equations of the example system

As an example we consider the dynamics of a horizontal taut cable, shown schematically in Fig. 1. This is described using the modal equations of motion, derived in [16] and discussed in detail in [4], which include gravitational sag and tension effects. The dynamics for the kth in- and out-of-plane modes, denoted z_k and y_k respectively (where in-plane relates to the plane in which gravitational sag occurs with the sag acting in the positive direction) may be expressed as

$$\ddot{z}_k+2\zeta_k\omega_{nk}\dot{z}_k+\omega_{nk}^2 z_k+\sum_{i=1}^{\infty}\frac{\nu_{ki}}{m}z_k(y_i^2+z_i^2)+\sum_{i=1}^{\infty}2\frac{\gamma_{ki}}{m}z_k z_i+\sum_{i=1}^{\infty}\frac{\gamma_{ik}}{m}(y_i^2+z_i^2)=0,$$

$$\ddot{y}_k+2\tilde{\zeta}_k\tilde{\omega}_{nk}\dot{y}_k+\tilde{\omega}_{nk}^2 y_k+\sum_{i=1}^{\infty}\frac{\nu_{ki}}{m}y_k(y_i^2+z_i^2)+\sum_{i=1}^{\infty}2\frac{\gamma_{ki}}{m}y_k z_i=\frac{2(-1)^k}{k\pi}\ddot{v}_\ell, \tag{4}$$

where it is assumed that an infinite number of modes exist in both the in-plane and out-of-plane directions. We note that k denotes the mode number, but for this structure there are two modes corresponding to each mode number: the kth in-plane, and the kth out-of-plane mode, as is reflected in the equations above. Here we use tilde, $\tilde{\bullet}$, to denote an out-of-plane parameter, and later it is also used to distinguish the out-of-plane modal variables. Linear modal damping is assumed, with damping ratios ζ_k and $\tilde{\zeta}_k$ for the kth in- and out-of-plane modes respectively. It can also be seen that forcing takes the form of an out-of-plane support motion, v_ℓ, at the $x=\ell$ support, where ℓ is the distance between supports. The parameter m describes the modal mass, and the nonlinear parameters γ_{ik} and ν_{ik} arise from the gravitational sag and from the dynamic tension respectively. These nonlinear parameters are defined in [16] where it is shown that $\nu_{ik}=i^2k^2\nu_{11}$ and that, for even k, $\gamma_{ik}=0$.

The linear natural frequencies of the kth in- and out-of-plane modes are written ω_{nk} and $\tilde{\omega}_{nk}$ respectively. Note that, for all out-of-plane modes and the even in-plane modes, these natural frequencies are proportional to the mode number k, while the natural frequencies of the odd in-plane modes are slightly higher than the equivalent out-of-plane ones. These equations have been used, for example, to analyse the onset of internal resonance [17,18] and whirling motion [12].

Here we consider the interactions between the ath unforced in-plane mode and the bth forced out-of-plane mode of the cable. Using $\mathbf{q}=(z_a\ \ y_b)^{\mathrm{T}}=(q_a\ \ \tilde{q}_b)^{\mathrm{T}}$, where the tilde notation is again used to denote the out-of-plane modes, the equations of motion for these two modes may be written in the matrix form of Eq. (1) with

$$\Gamma=\begin{bmatrix}2\zeta_a\omega_{na} & 0\\ 0 & 2\tilde{\zeta}_b\tilde{\omega}_{nb}\end{bmatrix},\quad \Lambda=\begin{bmatrix}\omega_{na}^2 & 0\\ 0 & \tilde{\omega}_{nb}^2\end{bmatrix},\quad \mathbf{f}=\frac{1}{m}\begin{pmatrix}0\\ R_b\Omega^2\cos(b\Omega t)\end{pmatrix},$$

$$\mathbf{N}(\mathbf{q})=\frac{1}{m}\begin{pmatrix}\nu_{aa}q_a^3+\nu_{ab}q_a\tilde{q}_b^2+3\gamma_{aa}q_a^2+\gamma_{ba}\tilde{q}_b^2\\ \nu_{ba}q_a^2\tilde{q}_b+\nu_{bb}\tilde{q}_b^3+2\gamma_{ba}q_a\tilde{q}_b\end{pmatrix}, \tag{5}$$

where it has been assumed that the support motion is sinusoidal, such that $v_\ell=V\cos(b\Omega t)$, and hence $R_b=-m\frac{2(-1)^b}{\pi}bV$. Additionally, it is assumed that $b\Omega$ is close to the out-of-plane linear natural frequency $\tilde{\omega}_{nb}$ and so may be treated as resonant.

As part of the normal form technique, we write $\mathbf{N}$ as a function of $\mathbf{u}$, rather than of $\mathbf{q}$ – see [5] for further details. Therefore, using $u_k=u_{pk}+u_{mk}$, gives

$$\mathbf{N}(\mathbf{u})=\frac{1}{m}\begin{pmatrix}\nu_{aa}(u_{pa}+u_{ma})^3+\nu_{ab}(u_{pa}+u_{ma})(\tilde{u}_{pb}+\tilde{u}_{mb})^2+3\gamma_{aa}(u_{pa}+u_{ma})^2+\gamma_{ba}(\tilde{u}_{pb}+\tilde{u}_{mb})^2\\ \nu_{ba}(u_{pa}+u_{ma})^2(\tilde{u}_{pb}+\tilde{u}_{mb})+\nu_{bb}(\tilde{u}_{pb}+\tilde{u}_{mb})^3+2\gamma_{ba}(u_{pa}+u_{ma})(\tilde{u}_{pb}+\tilde{u}_{mb})\end{pmatrix}. \tag{6}$$

From this we can express $\mathbf{N}(\mathbf{u})$ as the matrix multiplication $\mathbf{N}(\mathbf{u})=\mathbf{n}^*\mathbf{u}^*$ and calculate $\boldsymbol{\beta}^*$ using Eq. (A.1) to give

$$(\mathbf{n}^*)^{\mathsf{T}}=\frac{1}{m}\begin{bmatrix}\nu_{aa}&0\\3\nu_{aa}&0\\0&\nu_{ba}\\0&\nu_{ba}\\3\nu_{aa}&0\\0&2\nu_{ba}\\0&2\nu_{ba}\\\nu_{ab}&0\\2\nu_{ab}&0\\\nu_{ab}&0\\\nu_{aa}&0\\0&\nu_{ba}\\0&\nu_{ba}\\\nu_{ab}&0\\2\nu_{ab}&0\\\nu_{ab}&0\\0&\nu_{bb}\\0&3\nu_{bb}\\0&3\nu_{bb}\\0&\nu_{bb}\\3\gamma_{aa}&0\\6\gamma_{aa}&0\\0&2\gamma_{ba}\\0&2\gamma_{ba}\\3\gamma_{aa}&0\\0&2\gamma_{ba}\\0&2\gamma_{ba}\\\gamma_{ba}&0\\2\gamma_{ba}&0\\\gamma_{ba}&0\end{bmatrix},\quad \mathbf{u}^*=\begin{bmatrix}u_{pa}^3\\u_{pa}^2u_{ma}\\u_{pa}^2\tilde{u}_{pb}\\u_{pa}^2\tilde{u}_{mb}\\u_{pa}u_{ma}^2\\u_{pa}u_{ma}\tilde{u}_{pb}\\u_{pa}u_{ma}\tilde{u}_{mb}\\u_{pa}\tilde{u}_{pb}^2\\u_{pa}\tilde{u}_{pb}\tilde{u}_{mb}\\u_{pa}\tilde{u}_{mb}^2\\u_{ma}^3\\u_{ma}^2\tilde{u}_{pb}\\u_{ma}^2\tilde{u}_{mb}\\u_{ma}\tilde{u}_{pb}^2\\u_{ma}\tilde{u}_{pb}\tilde{u}_{mb}\\u_{ma}\tilde{u}_{mb}^2\\\tilde{u}_{pb}^3\\\tilde{u}_{pb}^2\tilde{u}_{mb}\\\tilde{u}_{pb}\tilde{u}_{mb}^2\\\tilde{u}_{mb}^3\\u_{pa}^2\\u_{pa}u_{ma}\\u_{pa}\tilde{u}_{pb}\\u_{pa}\tilde{u}_{mb}\\u_{ma}^2\\u_{ma}\tilde{u}_{pb}\\u_{ma}\tilde{u}_{mb}\\\tilde{u}_{pb}^2\\\tilde{u}_{pb}\tilde{u}_{mb}\\\tilde{u}_{mb}^2\end{bmatrix},\quad (\boldsymbol{\beta}^*)^{\mathsf{T}}=\Omega^2\begin{bmatrix}8a^2&-\\0&-\\-&4a(a+b)\\-&4a(a-b)\\0&-\\-&0\\-&0\\4b(a+b)&-\\0&-\\4b(b-a)&-\\8a^2&-\\-&4a(a-b)\\-&4a(a+b)\\4b(b-a)&-\\0&-\\4b(b+a)&-\\-&8b^2\\-&0\\-&0\\-&8b^2\\3a^2&-\\-a^2&-\\-&a(a+2b)\\-&a(a-2b)\\3a^2&-\\-&a(a-2b)\\-&a(a+2b)\\4b^2-a^2&-\\-a^2&-\\4b^2-a^2&-\end{bmatrix}. \tag{7}$$

Here we have written the response frequencies as $\omega_{ra}=a\Omega$ and $\tilde{\omega}_{rb}=b\Omega$, recalling that $\Omega=2\pi/T$, where T is the period of the response. The elements in $\boldsymbol{\beta}^*$ containing dashes are not needed as they correspond to elements in $\mathbf{n}^*$ with a value of zero.

From this expression for $\boldsymbol{\beta}^*$ it can be seen that some terms are zero regardless of the values of a and b, these are referred to as *unconditionally resonant terms* [11]. In addition, there are *conditionally resonant terms*, which are zero if a relationship between a and b is met. From inspection of $\boldsymbol{\beta}^*$ it can be seen that conditionally resonant terms occur if $a=b$ (elements [1, 10], [1, 14], [2, 4] and [2, 12]) or if $a=2b$ (elements [1, 28], [1, 30], [2, 24] and [2, 26]). However for the case where $a=2b$, the corresponding values in $\mathbf{n}^*$ are all a function ofγ_{ba} which is zero if a is even, as it must be to satisfy $a=2b$. Hence $a=2b$ does not result in non-zero conditionally resonant terms.

To proceed, therefore, we consider two cases; (i) the case where $a=b$ which contains conditionally resonant terms and (ii) the more general case where $a\neq b$ which only contains unconditionally resonant terms. Keeping the resonant terms in the equation of motion and removing the non-resonant ones using the $\mathbf{q}\rightarrow\mathbf{u}$ transform results in the resonant equation of motion $\ddot{\mathbf{u}}+\Gamma\dot{\mathbf{u}}+\Lambda\mathbf{u}+\mathbf{N}_u(\mathbf{u})=\mathbf{f}$ where

$$\mathbf{N}_u(\mathbf{u})=\frac{1}{m}\begin{pmatrix}3\nu_{aa}u_{pa}u_{ma}u_a+2\nu_{ab}\tilde{u}_{pb}\tilde{u}_{mb}u_a+\delta_{a,b}\nu_{ab}\left(u_{pa}\tilde{u}_{mb}^2+u_{ma}\tilde{u}_{pb}^2\right)\\2\nu_{ba}u_{pa}u_{ma}\tilde{u}_b+3\nu_{bb}\tilde{u}_{pb}\tilde{u}_{mb}\tilde{u}_b+\delta_{a,b}\nu_{ba}\left(u_{pa}^2\tilde{u}_{mb}+u_{ma}^2\tilde{u}_{pb}\right)\end{pmatrix}, \tag{8}$$

and where $\delta_{a,b}$ is the Kronecker Delta function, where $\delta_{a,b}=0$ when $a\neq b$, and $\delta_{a,b}=1$ when $a=b$.

3. Backbone curves

To calculate the backbone curves, the trial solution, Eq. (2), is substituted into the unforced, undamped equations of motion, $\ddot{\mathbf{u}}+\Lambda\mathbf{u}+\mathbf{N}_u(\mathbf{u})=0$. Making this substitution into the kth equation, $\ddot{u}_k+\omega_{nk}^2u_k+N_{uk}(\mathbf{u})=0$, and balancing the $e^{\mathbf{j}\omega_{rk}t}$ terms gives

$$U_k(\omega_{nk}^2-\omega_{rk}^2)+2N_{uk}^+e^{\mathbf{j}\phi_k t}=0, \tag{9}$$

where, making use of the fact that the transformed dynamic equation contains only resonant terms, we have written

$$N_{uk}(\mathbf{u})=N_{uk}^+e^{\mathbf{j}\omega_{rk}t}+N_{uk}^-e^{-\mathbf{j}\omega_{rk}t}. \tag{10}$$

Note that balancing the $e^{-\mathbf{j}\omega_{rk}t}$ gives the complex conjugate of this expression and so offers no extra information when used to compute a solution. The imaginary parts of these equations (for $1\le k\le n$, where n is the number of modes) may be used to find any phase conditions between the modes. The real parts may then be solved to find expressions for the backbone curves.

In the case of the cable example, Eq. (9) may be written as

$$\left\{\omega_{na}^2-\omega_{ra}^2+\frac{1}{4m}\left[3\nu_{aa}U_a^2+2\nu_{ab}\tilde{U}_b^2+\delta_{a,b}\nu_{ab}\tilde{U}_b^2e^{2\mathbf{j}\left(\phi_a-\tilde{\phi}_b\right)}\right]\right\}U_a=0, \tag{11}$$

$$\left\{\tilde{\omega}_{nb}^2-\tilde{\omega}_{rb}^2+\frac{1}{4m}\left[2\nu_{ba}U_a^2+3\nu_{bb}\tilde{U}_b^2+\delta_{a,b}\nu_{ba}U_a^2e^{2\mathbf{j}\left(\tilde{\phi}_b-\phi_a\right)}\right]\right\}\tilde{U}_b=0. \tag{12}$$

For the general case, $a\neq b$, there is no phase relationship imposed by the equations of motion (as the Kronecker delta functions set the imaginary parts of Eq. (9) to zero) and we have the amplitude–response frequency expressions

$$\text{for } a\neq b:\quad \left\{\omega_{na}^2-\omega_{ra}^2+\frac{1}{4m}\left[3\nu_{aa}U_a^2+2\nu_{ab}\tilde{U}_b^2\right]\right\}U_a=0, \tag{13}$$

$$\left\{\tilde{\omega}_{nb}^2-\tilde{\omega}_{rb}^2+\frac{1}{4m}\left[2\nu_{ba}U_a^2+3\nu_{bb}\tilde{U}_b^2\right]\right\}\tilde{U}_b=0. \tag{14}$$

Recall that, for a single frequency resonant response, $\Omega=\omega_{ra}/a=\tilde{\omega}_{rb}/b$. However for the special case where $a=b$, to satisfy the imaginary part of Eq. (9), the phase condition $\sin\left[2\left(\tilde{\phi}_a-\phi_a\right)\right]=0$ must be met. This leads to either the phase relationship $\tilde{\phi}_a-\phi_a=0,\pi,\ldots$ with $e^{2\mathbf{j}\left(\tilde{\phi}_a-\phi_a\right)}=1$ or $\tilde{\phi}_a-\phi_a=\pi/2,3\pi/2,\ldots$ with $e^{2\mathbf{j}\left(\tilde{\phi}_a-\phi_a\right)}=-1$. Hence, we say that the modes are *phase-locked* when

$$\text{for } a=b:\quad \left\{\omega_{na}^2-a^2\Omega^2+\frac{\nu_{aa}}{4m}\left[3U_a^2+(2+p)\tilde{U}_a^2\right]\right\}U_a=0, \tag{15}$$

$$\left\{\tilde{\omega}_{na}^2-a^2\Omega^2+\frac{\nu_{aa}}{4m}\left[(2+p)U_a^2+3\tilde{U}_a^2\right]\right\}\tilde{U}_a=0, \tag{16}$$

where $p=1$ if the modes are in-phase or in anti-phase, $\tilde{\phi}_a-\phi_a=0,\pi$, and $p=-1$ if the modes are out-of-phase, $\tilde{\phi}_a-\phi_a=\pi/2,3\pi/2$.

We find that there are two single-mode backbone solutions, which are independent of the relationship between modes a and b. These backbone curves are also independent of p, which only appears in mixed-mode terms. By inspection of Eqs. (13) and (14) and of Eqs. (15) and (16), these solutions (in terms of the resonant response) are the in-plane-only mode

$$S1:\quad \tilde{U}_b=0,\quad a^2\Omega^2=\omega_{na}^2+\frac{3\nu_{aa}}{4m}U_a^2, \tag{17}$$

and the out-of-plane-only mode

$$S2:\quad U_a=0,\quad b^2\Omega^2=\tilde{\omega}_{nb}^2+\frac{3\nu_{bb}}{4m}\tilde{U}_b^2. \tag{18}$$

In addition to these, there are mixed-mode solutions. To find these, firstly the special case of $a=b$ will be considered followed by the general case $a\neq b$.

3.1. The phase-locked case: $a=b$

Taking the case where $a=b$, U_a and $\tilde{U}_a$ denote the amplitudes of the in- and out-of-plane modes respectively. There are potentially four types of solution, as has been discussed for the case where $a=b=1$ in [12]: two single-mode solutions, $S1$ and $S2$; and two mixed-mode solutions. These mixed-mode solutions may be found by setting the contents of the bracketed terms in Eqs. (15) and (16) to zero and eliminating the response frequency giving the amplitude relationship

$$\frac{\nu_{aa}}{4m}(1-p)\left(\tilde{U}_a^2-U_a^2\right)=\omega_{na}^2-\tilde{\omega}_{na}^2\ge 0, \tag{19}$$

using the fact that $\omega_{na}\ge\tilde{\omega}_{na}$.

The case where $p=1$ can only give valid solutions if $\omega_{na}=\tilde{\omega}_{na}$, which occurs when a is even. In this case there is no relationship between the amplitudes of the two modes. Using Eq. (15), for this case we can write

$$S3^{\pm}_{a=b,\text{even } a}: \quad a^2\Omega^2=\omega_{na}^2+\frac{3\nu_{aa}}{4m}\left(U_a^2+\tilde{U}_a^2\right), \quad \text{for even } a, \tag{20}$$

where, for $S3^+$ and $S3^-$, the phase difference is $\tilde{\phi}_a-\phi_a=0$ and $\tilde{\phi}_a-\phi_a=\pi$ respectively. Note that, for even values of a, solutions $S1$ and $S2$ are special cases of solution $S3^{\pm}$. Physically, in a plane intersecting the chord line (see Fig. 1) we have a physical amplitude of oscillation at mid-span of $\sqrt{U_a^2+\tilde{U}_a^2}$ with a linear natural frequency of $\omega_{na}=\tilde{\omega}_{na}$.

Now considering the case where $p=-1$, from Eq. (19) we have

$$\frac{\nu_{aa}}{2m}\left(\tilde{U}_a^2-U_a^2\right)=\omega_{na}^2-\tilde{\omega}_{na}^2\geq 0. \tag{21}$$

Here, using Eqs. (15) and (16), the resonant frequency may be written as

$$S4^{\pm}_{a=b}: \quad a^2\Omega^2=\frac{\nu_{aa}}{2m}\left(\tilde{U}_a^2+U_a^2\right)+\frac{1}{2}\left(\omega_{na}^2+\tilde{\omega}_{na}^2\right)$$
$$\tilde{U}_a^2=U_a^2+\frac{2m}{\nu_{aa}}\left(\omega_{na}^2-\tilde{\omega}_{na}^2\right), \tag{22}$$

where for $S4^+$ and $S4^-$ the phase is $\tilde{\phi}_a-\phi_a=\pi/2$ and $\tilde{\phi}_a-\phi_a=-\pi/2$ respectively, such that the cable is whirling clockwise or anti-clockwise. Note that $U_a=0$ is a valid solution to Eq. (22), and in this case the solution lies on $S2$. This point represents a bifurcation between $S2$ and the whirling $S4^{\pm}$ solutions, see [12]. Note also for the case where a is even, such that $\omega_{na}=\tilde{\omega}_{na}$, $S4^{\pm}$ describes responses in which $U_a=\tilde{U}_a$ and the bifurcation occurs at zero-amplitude.

As an example, we now consider a cable with a length of 1.5 m, a diameter of 5 mm, a density of 3000 kg m^{-3}, Young's Modulus of 2×10^{11} Pa and a static tension of 200 N, as originally described in [12]. Fig. 2 shows the backbone curves for the case where $a=b=1$ for the first in- and out-of-plane modes. The non-zero $S1$ and $S2$ solutions are confined to U_1, panel (a), and $\tilde{U}_1$, panel (b), respectively. At approximately $\Omega=124.8$ rad s^{-1}, the mixed-mode backbone $S4^{\pm}$ bifurcates off the $S2$ solution branch with $U_1=0$, with increasing U_1 and $\tilde{U}_1$ away from the bifurcation point.

3.2. The phase-unlocked case: $a\neq b$

Considering the general case where $a\neq b$, Eqs. (13) and (14), we again have the two single-mode solutions $S1$ and $S2$ (Eqs. (17) and (18)). In addition, as with $a=b$, it is possible to have solutions where both modes are present. Taking Eqs. (13) and (14) and eliminating $\Omega=\omega_{rk}/k$ give

$$b^2\tilde{U}_b^2-a^2U_a^2=\frac{4m}{a^2\nu_{11}}\left(\omega_{na}^2-\frac{a^2}{b^2}\tilde{\omega}_{nb}^2\right), \tag{23}$$

where it has been recalled that $\nu_{ij}=i^2j^2\nu_{11}$. Note that $\omega_{na}\geq(a/b)\tilde{\omega}_{nb}$ so the bracketed term is positive or zero. Using this equation and Eq. (14) to calculate the resonant frequency, the mixed-mode solution may be summarised as

$$S5^{*}_{a\neq b}: \quad \tilde{\omega}_{rb}^2=\frac{b^2}{a^2}\omega_{ra}^2=\tilde{\omega}_{nb}^2+\frac{\nu_{11}b^2}{4m}\left(2a^2U_a^2+3b^2\tilde{U}_b^2\right)$$
$$\tilde{U}_b^2=\frac{a^2}{b^2}U_a^2+\frac{4m}{a^2b^2\nu_{11}}\left(\omega_{na}^2-\frac{a^2}{b^2}\tilde{\omega}_{nb}^2\right). \tag{24}$$

Note that there is no phase condition imposed on the modal contributions, this is indicated by the $*$ superscript. Here $U_a=0$ is a valid solution and at this point the solution lies on $S2$, hence this solution branch bifurcates from $S2$.

Fig. 3 shows the case where $a=1$ and $b=3$, in the projection of the response frequency, Ω, against the fundamental response amplitude of the third out-of-plane mode, $\tilde{U}_3$. It can be seen that it is qualitatively similar to the plot shown in

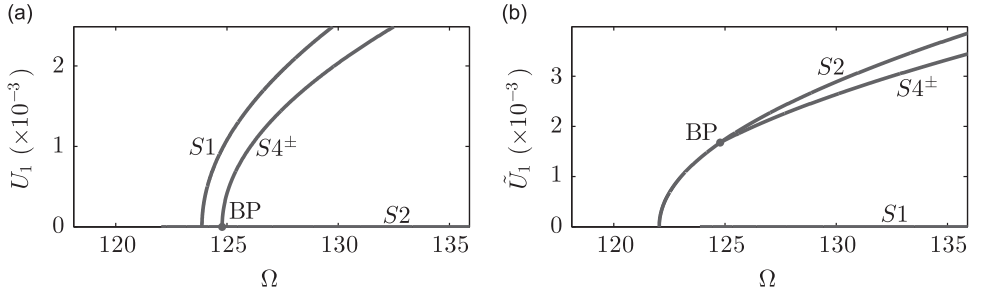

Fig. 2. Backbone curves for a two-mode cable model, considering the case where resonance occurs in either one linear mode, or in both. The resonant amplitudes are shown in terms of the linear modal contribution from (a) the first in-plane mode and (b) the first out-of-plane mode. These backbone curves are found using the parameters $m=0.04418$ kg, $\omega_{n1}=122.04$ rad s^{-1}, $\tilde{\omega}_{n1}=123.9$ rad s^{-1} and $\nu_{11}=1.417\times10^7$ kg m^{-2} s^{-2}.

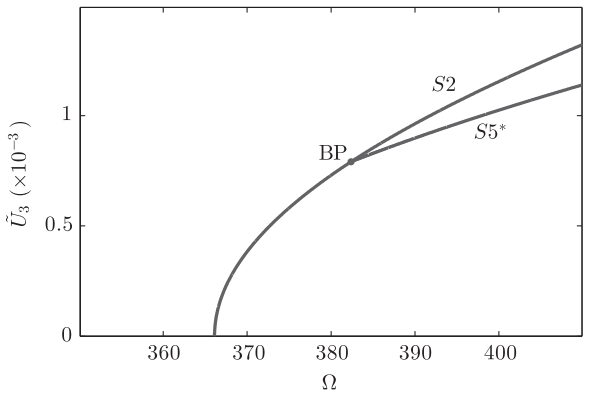

Fig. 3. Backbone curves for a cable, with parameters defined in [12], considering the case where resonance occurs in either or both of the first in-plane and third out-of-plane modes. These backbone curves are found using the parameters $m = 0.04418$ kg, $\omega_{n1} = 122.04$ rad s^{-1}, $\tilde{\omega}_{n3} = 366.1$ rad s^{-1} and $\nu_{11} = 1.417 \times 10^7$ kg m^{-2} s^{-2}.

panel (b) of Fig. 2, although it should be noted that on the $S5^*$ branch the corresponding response in the first in-plane mode, with response amplitude U_1, will be at one-third the frequency of the $\tilde{U}_3$ component. We note that, to get a full picture of the dynamic interactions in the cable, all combinations of modes must be considered; however here we show an example interaction between a pair of modes.

4. Internal resonance

Now we consider the potential for the system to exhibit internal resonance, i.e. to respond in a mode that is not directly excited. This will be achieved by considering the zero-amplitude response stability of an unforced mode. If the zero-amplitude response solution is unstable, due to the presence of another mode, then an internal resonance of the unforced mode will be observed. The findings will be applied to our example system by considering the response of the ath in-plane mode when the cable is excited out-of-plane close to the frequency of the bth out-of-plane mode. From the backbone analysis, it is revealed that the two-mode cable system is likely to exhibit internal resonance due to the presence of mixed-mode backbone curves. This potential internal resonance is examined by considering the stability of the zero-amplitude response solution to the ath in-plane mode.

To assess the stability of the zero-solution of an unforced mode in a general system, we must consider the response of the mode when subjected to a perturbation away from zero. This is achieved by allowing the amplitude and phase of the response to vary slowly in time which, for the kth mode, may be expressed using

$$u_k = u_{pk} + u_{mk} = \frac{U_{pk}(\varepsilon t)}{2} e^{\mathbf{j}\omega_{rk}t} + \frac{U_{mk}(\varepsilon t)}{2} e^{-\mathbf{j}\omega_{rk}t}, \tag{25}$$

where, from comparison with Eq. (2), $U_{pk} = U_k e^{-\mathbf{j}\phi_k}$ and $U_{mk} = U_k e^{\mathbf{j}\phi_k}$. Here we have two time-scales: the oscillatory motion at frequency ω_{rk}, and a slowly varying amplitude represented by the amplitude dependence on εt where ε is a bookkeeping aid [19] used to indicate a small parameter (and may be removed at an appropriate stage by setting it to unity). The use of this type of solution is discussed at length in [4,11]. Using a fast- and slow-time approach the derivatives of this solution can be written as

$$\begin{aligned} \dot{u}_{pk} &= \frac{1}{2}\mathbf{j}\omega_{rk}U_{pk}e^{\mathbf{j}\omega_{rk}t}, \quad \dot{u}_{mk} = -\frac{1}{2}\mathbf{j}\omega_{rk}U_{mk}e^{-\mathbf{j}\omega_{rk}t}, \\ \ddot{u}_{pk} &= \left(-\frac{\omega_{rk}^2}{2}U_{pk} + \mathbf{j}\omega_{rk}\dot{U}_{pk}\right)e^{\mathbf{j}\omega_{rk}t}, \quad \ddot{u}_{mk} = \left(-\frac{\omega_{rk}^2}{2}U_{mk} - \mathbf{j}\omega_{rk}\dot{U}_{mk}\right)e^{-\mathbf{j}\omega_{rk}t}. \end{aligned} \tag{26}$$

Here the first derivatives are expressed to order ε^0 as they will only be used in small terms in the equations of motion (damping is assumed to be small), whereas the second derivatives are expressed to order ε^1 as they will be used in large terms, hence preserving the accuracy of the solution to order ε^1.

To proceed, this solution is substituted into the resonant equation of motion for an unforced mode $\ddot{u}_k + 2\zeta_k\omega_{nk}\dot{u}_k + \omega_{nk}^2 u_k + N_{uk}(\mathbf{u}) = 0$, and then the $e^{\mathbf{j}\omega_{rk}t}$ and $e^{-\mathbf{j}\omega_{rk}t}$ terms in the resulting equation are balanced (as the equation is resonant there are no other complex exponential terms in time so this balance is exact) to give

$$\begin{aligned} \dot{U}_{pk} &= \frac{1}{2\omega_{rk}}\left[\mathbf{j}\left(\left[\omega_{nk}^2 - \omega_{rk}^2\right]U_{pk} + 2N_{uk}^{+}(\mathbf{u})\right) - 2\zeta_k\omega_{nk}\omega_{rk}U_{pk}\right], \\ \dot{U}_{mk} &= \frac{1}{2\omega_{rk}}\left[-\mathbf{j}\left(\left[\omega_{nk}^2 - \omega_{rk}^2\right]U_{mk} + 2N_{uk}^{-}(\mathbf{u})\right) - 2\zeta_k\omega_{nk}\omega_{rk}U_{mk}\right]. \end{aligned} \tag{27}$$

Expressing this in the form $\dot{\mathbf{z}} = f(\mathbf{z}, t)$ where $\mathbf{z} = \{U_{pk}\ \ U_{mk}\}^{\mathrm{T}}$, steady-state solutions, $\mathbf{z}_s$, may be found by solving $f(\mathbf{z}_s, t) = 0$. The stability of these steady-state solutions may be assessed, to the first order of accuracy of a Taylor series expansion, by examining the eigenvalues of $Df_z(\mathbf{z}_s, t)$, where $Df_z(\mathbf{z}, t)$ is the Jacobian of $f(\mathbf{z}, t)$; if the real part of the eigenvalues are positive then the solution is unstable, see for example [4]. Using Eq. (27), the Jacobian may be expressed as

$$Df_z(\mathbf{z}, t) = \frac{1}{2\omega_{rk}} \times \begin{pmatrix} \mathbf{j}(\omega_{nk}^2 - \omega_{rk}^2 + 2\partial N_{uk}^+/\partial U_{pk}) - 2\zeta_k\omega_{nk}\omega_{rk} & \mathbf{j}2\partial N_{uk}^+/\partial U_{mk} \\ -\mathbf{j}2\partial N_{uk}^-/\partial U_{pk} & -\mathbf{j}(\omega_{nk}^2 - \omega_{rk}^2 + 2\partial N_{uk}^-/\partial U_{mk}) - 2\zeta_k\omega_{nk}\omega_{rk} \end{pmatrix}, \tag{28}$$

where we have used Eq. (10) to reflect that fact that $N_{uk}(\mathbf{u})$ has $\mathrm{e}^{\mathbf{j}\omega_{rk}t}$ and $\mathrm{e}^{-\mathbf{j}\omega_{rk}t}$ terms. Since we are interested in the zero-amplitude response solution, we need to set $\mathbf{z} = \mathbf{z}_s = [0\ \ 0]^{\mathrm{T}}$. Additionally, it can be assumed that the perturbed solution is small, and hence any terms containing $U_{pk}^i U_{mk}^j$ where $i+j > 1$ are considered to be negligible.

4.1. The form of the resonant nonlinearities

Before proceeding, it is worth considering further the form of $N_{uk}(\mathbf{u})$. Firstly, we know that all terms contain at least one U_{pk}^1 or U_{mk}^1 term, otherwise the zero-amplitude response solution would not exist. Secondly, we know that these terms are resonant, but, considering Eq. (A.1), we can see that there are two ways of satisfying this: either via a positive or a negative root. We also know that the higher order terms of $[U_{pk},\ U_{mk}]$ do not need to be considered in the stability assessment as they disappear when evaluating the Jacobian for $\mathbf{z} = \mathbf{z}_s = [0\ \ 0]^{\mathrm{T}}$. Finally, we know that $N_{uk}(\mathbf{u})$ is real.

Considering a multimode system with the zero-amplitude response solution in mode k, which has resonant frequency $\omega_{rk} = r_k\Omega$, there are four possible types of resonant term which are functions of either U_{pk}^1 or U_{mk}^1, these are

$$p1: \quad u_{pk}\prod_{i,i\neq k} u_{pi}^{s_{pi}} u_{mi}^{s_{mi}} \quad \text{with:} \sum_{i,i\neq k} r_i(s_{pi} - s_{mi}) = 0, \tag{29}$$

$$p2: \quad u_{pk}\prod_{i,i\neq k} u_{pi}^{s_{pi}} u_{mi}^{s_{mi}} \quad \text{with:} \sum_{i,i\neq k} r_i(s_{pi} - s_{mi}) = -2r_k, \tag{30}$$

$$p3: \quad u_{mk}\prod_{i,i\neq k} u_{pi}^{s_{pi}} u_{mi}^{s_{mi}} \quad \text{with:} \sum_{i,i\neq k} r_i(s_{pi} - s_{mi}) = 2r_k, \tag{31}$$

$$p4: \quad u_{mk}\prod_{i,i\neq k} u_{pi}^{s_{pi}} u_{mi}^{s_{mi}} \quad \text{with:} \sum_{i,i\neq k} r_i(s_{pi} - s_{mi}) = 0. \tag{32}$$

Possibilities $p1$ and $p4$ place no condition on the response frequency ω_{rk} and hence are phase-unlocked terms with respect to the kth mode. They also result in a positive and negative complex exponential in time for the u_{pk} and u_{mk} terms respectively, and so appear in the leading-diagonal terms of the Jacobian. Furthermore, as these terms may be written $N_{uk}^u u_k$, where N_{uk}^u is time-independent, it may be seen that N_{uk}^u must be real. In contrast, $p2$ and $p3$ require a frequency relationship between the kth mode and the other modes in the system. Using Eq. (2), this results in a phase of the nonlinear term, relative to the linear term, of $-2\phi_k + \sum_{i,i\neq k}[\phi_i(s_{pi} - s_{mi})] = n\pi$ for both solutions. As $p2$ is a negative complex exponential in time and $p3$ a positive one, these phase-locked terms will appear in the off-diagonals of the Jacobian, and these terms form a complex conjugate pair, ensuring that $N_{uk}(\mathbf{u})$ is real.

Using the response solution given by Eq. (25), this allows us to write

$$N_{uk}(\mathbf{u}) = N_{uk}^u U_{pk}\mathrm{e}^{\mathbf{j}\omega_{rk}t} + N_{uk}^u U_{mk}\mathrm{e}^{-\mathbf{j}\omega_{rk}t} + N_{uk}^l U_{pk}\mathrm{e}^{-\mathbf{j}\omega_{rk}t} + \overline{N}_{uk}^l U_{mk}\mathrm{e}^{\mathbf{j}\omega_{rk}t} + \text{h.o.t}\ ., \tag{33}$$

where superscripts u and l indicate phase-unlocked and locked terms respectively, and the overbar indicates the complex conjugate, and we note that N_{uk}^u is real. Additionally, note that these terms are in the order $p1$, $p4$, $p2$ and $p3$.

Using this, the form of the resonant nonlinearities allows the Jacobian matrix, Eq. (28), to be rewritten as

$$Df_z(\mathbf{z}, t) = \frac{1}{2\omega_{rk}} \times \begin{pmatrix} \mathbf{j}(\omega_{nk}^2 - \omega_{rk}^2 + 2N_{uk}^u) - 2\zeta_k\omega_{nk}\omega_{rk} & \mathbf{j}2N_{uk}^l \\ -\mathbf{j}2\overline{N}_{uk}^l & -\mathbf{j}(\omega_{nk}^2 - \omega_{rk}^2 + 2N_{uk}^u) - 2\zeta_k\omega_{nk}\omega_{rk} \end{pmatrix}. \tag{34}$$

4.2. Zero-amplitude response stability

Using the form of the resonant nonlinearities given in Eq. (33) the eigenvalues of the Jacobian matrix may be written as

$$(2\omega_{rk}\lambda)^2 + 4\zeta_k\omega_{nk}\omega_{rk}(2\omega_{rk}\lambda) + 4\zeta_k^2\omega_{nk}^2\omega_{rk}^2 + (\omega_{nk}^2 - \omega_{rk}^2 + 2N_{uk}^u)^2 - 4N_{uk}^l\overline{N}_{uk}^l = 0. \tag{35}$$

It follows that for the real part of an eigenvalue, λ, to be positive we require

$$4\zeta_k^2\omega_{nk}^2\omega_{rk}^2 + (\omega_{nk}^2 - \omega_{rk}^2 + 2N_{uk}^u)^2 \leq 4N_{uk}^l\overline{N}_{uk}^l. \tag{36}$$

This implies that a necessary, but not sufficient, requirement for an unstable zero-amplitude response solution for the kth mode is that N^l_{uk} must be non-zero. Hence, for the triggering of a response in an unforced mode, phase-locked terms are required.

4.3. Application to the cable example

Now, considering the cable example when the bth out-of-plane mode is excited directly, we determine whether the ath in-plane mode may respond via internal resonance. Using the first line in Eq. (8), along with Eqs. (25) and (33), we can write

$$N^u_{ua}=\frac{\nu_{ab}}{4m}\tilde{U}_{pb}\tilde{U}_{mb},\quad N^l_{ua}=\frac{\nu_{ab}}{8m}\delta_{a,b}\tilde{U}^2_{pb},\quad \overline{N}^l_{ua}=\frac{\nu_{ab}}{8m}\delta_{a,b}\tilde{U}^2_{mb}. \tag{37}$$

Considering Eq. (36) it can be seen that an unstable zero-amplitude response solution for the bth mode can only exist when $a=b$. Therefore, for $a\neq b$, while we have calculated mixed-mode backbone curves (solutions $S5^*_{a\neq b}$), no internally resonant forced response along these backbone curves will be observed. For the case where $a=b$, using Eq. (36), the point of instability of zero-amplitude response solution of the ath in-plane mode, i.e. the point at which a response of the in-plane mode is triggered, occurs when the forced response solution of the ath out-of-plane mode crosses the resonant tongue defined by

$$4\zeta^2_a\omega^2_{na}\omega^2_{ra}+\left(\omega^2_{na}-\omega^2_{ra}+\frac{\nu_{aa}}{2m}\tilde{U}^2_a\right)^2=\frac{\nu^2_{aa}}{16m^2}\tilde{U}^4_a, \tag{38}$$

where we have noted that $\tilde{U}_{pa}\tilde{U}_{ma}=\tilde{U}^2_a$ by comparing Eqs. (2) and (25).

Note that in the cable analysis we could have considered the forcing of many out-of-plane modes. This would have shown that the ith in-plane modes can only be triggered, but will not necessarily be triggered, by a response in the ith out-of-plane mode as it is just this mode which provides a phase-locked coupling. It is also interesting to note that there are no phase-locked terms between different in-plane or between different out-of-plane modes (the equations take the same form as between an in- and an out-of-plane mode). A special case is when the cable is inclined, when additional parametric forcing terms are introduced due to the inclination, allowing a 1:2 resonance, see for example [17,18].

Fig. 4(a) shows the forced response of the cable due to out-of-plane support excitation when the first in-plane and the first out-of-plane modes are considered. For this, and subsequent figures, the forced response was calculated using numerical continuation, whereas the backbone curves were generated from the analytical solutions derived earlier. Note that forced responses may also be found analytically using the second-order normal form technique – see, for example, [5,14]. Here, however, numerical continuation is employed to validate the assumptions used to find the backbone curves.

The transitions between the white and the green background to Fig. 4(a) mark the resonant tongue, given by Eq. (38). The points at which the primary forced response curve, containing only the out-of-plane mode, meets this boundary, coincide with bifurcation points. An additional branch, containing both the in- and out-of-plane modes, emerges from these bifurcation points and envelops the $S4^{\pm}$ backbone. In the case of the upper bifurcation point, it can be seen that the solution following $S2$ becomes unstable at the bifurcation, indicating the loss of stability of the zero-amplitude response solution of the in-plane mode. In contrast, for the case where the first in-plane and the third out-of-plane modes are considered, Fig. 4 (b), there is no resonant tongue, and the response envelops $S2$ throughout.

5. Stiffening effects

We have seen that, to observe internal resonance between a forced and an unforced mode, phase-locking resonant terms are necessary but not sufficient. In the case of the cable example such terms only exist between the kth in- and kth out-of-plane modes. The resulting motion envelops a mixed-mode backbone curve (or NNM branch), namely the $S4^{\pm}$ solution branch for the cable example. We now consider the effect of other modes on the onset of internal resonance between a forced and an unforced mode that have phase-locking resonant terms. For this discussion we consider the cable example and, specifically, we investigate the influence of an additional out-of-plane mode that is subjected to near-resonant forcing.

The cth out-of-plane mode may experience near-resonant excitation when the support motion is $v_\ell=V_b\cos(b\Omega t)+V_c\cos(c\Omega t)$. From Eq. (4), this leads to the modal equations of motion, written

$$\begin{aligned}
&m(\ddot{q}_a+2\zeta_a\omega_{na}\dot{q}_a+\omega^2_{na}q_a)+\nu_{aa}q^3_a+\nu_{ab}q_a\tilde{q}^2_b+\nu_{ac}q_a\tilde{q}^2_c+3\gamma_{aa}q^2_a+\gamma_{ba}\tilde{q}^2_b+\gamma_{ca}\tilde{q}^2_c=0,\\
&m\left(\ddot{\tilde{q}}_b+2\tilde{\zeta}_b\tilde{\omega}_{nb}\dot{\tilde{q}}_b+\tilde{\omega}^2_{nb}\tilde{q}_b\right)+\nu_{ba}q^2_a\tilde{q}_b+\nu_{bb}\tilde{q}^3_b+\nu_{bc}\tilde{q}_b\tilde{q}^2_c+2\gamma_{ba}q_a\tilde{q}_b=R_{bb}\Omega^2\cos(b\Omega t)+R_{bc}\Omega^2\cos(c\Omega t),\\
&m\left(\ddot{\tilde{q}}_c+2\tilde{\zeta}_c\tilde{\omega}_{nc}\dot{\tilde{q}}_c+\tilde{\omega}^2_{nc}\tilde{q}_c\right)+\nu_{ca}q^2_a\tilde{q}_c+\nu_{cb}\tilde{q}^2_b\tilde{q}_c+\nu_{cc}\tilde{q}^3_c+2\gamma_{ca}q_a\tilde{q}_c=R_{cb}\Omega^2\cos(b\Omega t)+R_{cc}\Omega^2\cos(c\Omega t),
\end{aligned} \tag{39}$$

where $R_{ij}=-m\frac{2(-1)^i}{i\pi}j^2V_j$, and where, from Eq. (4), $q_a=z_a$, $\tilde{q}_b=y_b$ and $\tilde{q}_c=y_c$.

To fully apply the normal form technique to the forced system requires a forcing transform, $\mathbf{q}=\mathbf{v}+\mathbf{e}$, prior to the nonlinear transform, $\mathbf{u}=\mathbf{v}+\mathbf{h}$, [20,15]. This transform removes non-resonant forcing terms from each modal equation, by introducing parametric excitation terms into the nonlinear vector. However, a first approximation is to assume that the out-

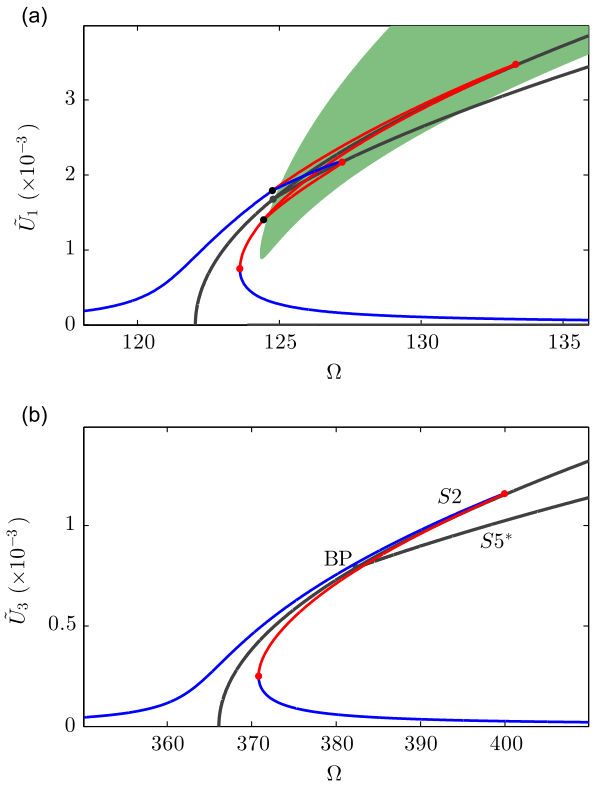

Fig. 4. Forced response of the cable using a two-mode model consisting of the ath in-plane mode and the bth out-of-plane mode, where (a) $a=b=1$ and (b) $a=1$ and $b=3$. Backbone curves are shown in dark grey, stable and unstable forced responses are shown in blue and red respectively and the loss of stability of the zero-amplitude response solution for the in-plane mode is shown as a transition between the white and the green backgrounds. These backbone curves correspond to those shown in Figs. 2 and 3, and are computed using the parameters $m=0.04418$ kg, $\omega_{n1}=122.04$ rad s^{-1}, $\tilde{\omega}_{n1}=123.9$ rad s^{-1}, $\tilde{\omega}_{n3}=366.1$ rad s^{-1} and $\nu_{11}=1.417\times10^{7}$ kg m^{-2} s^{-2}. Additionally, to compute the forced responses, the nonlinear parameter values $\gamma_{11}=1.188\times10^{4}$ kg m^{-1} s^{-2} and $\gamma_{31}=1.069\times10^{5}$ kg m^{-1} s^{-2} are used. In both forcing cases, the modal damping is $\zeta_1=\tilde{\zeta}_1=\tilde{\zeta}_3=0.002$ and the amplitude of displacement of the support is $V=0.02$ mm. (For interpretation of the references to colour in this figure caption, the reader is referred to the web version of this paper.)

of-plane response terms are large compared to the forcing terms and so $\mathbf{e}$ can be neglected when compared to $\mathbf{v}$. This allows us to find, albeit approximate, solutions using the analysis outlined in the previous sections.

Using this approximation, we now consider how the presence of the cth out-of-plane mode influences the modal interactions between the ath in-plane and bth out-of-plane modes (where $a=b$). The analysis used to identify the NNMs relating to the ath in-plane and bth out-of-plane modes is modified to include terms due to the presence of the directly excited cth out-of-plane mode, due to the $\nu_{ac}q_a\tilde{q}_c^2$ and $\nu_{bc}\tilde{q}_b\tilde{q}_c^2$ terms in the equations of motion. Redefining the resonant response vector as $\mathbf{u}=[u_a\ \tilde{u}_b\ \tilde{u}_c]^\top=[u_a\ \tilde{u}_a\ \tilde{u}_c]^\top$, the vector containing the resonant nonlinear terms for the three modes, formerly Eq. (8), is given by

$$\mathbf{N}_u(\mathbf{u})=\frac{1}{m}\begin{pmatrix} 3\nu_{aa}u_{pa}u_{ma}u_a+\nu_{aa}\left(2\tilde{u}_{pa}\tilde{u}_{ma}u_a+u_{pa}\tilde{u}_{ma}^2+u_{ma}\tilde{u}_{pa}^2\right)+2\nu_{ac}\tilde{u}_{pc}\tilde{u}_{mc}u_a \\ \nu_{aa}\left(2u_{pa}u_{ma}\tilde{u}_a+u_{pa}^2\tilde{u}_{ma}+u_{ma}^2\tilde{u}_{pa}\right)+3\nu_{aa}\tilde{u}_{pa}\tilde{u}_{ma}\tilde{u}_a+2\nu_{ac}\tilde{u}_{pc}\tilde{u}_{mc}\tilde{u}_a \\ 2\nu_{ca}u_{pa}u_{ma}\tilde{u}_c+2\nu_{ca}\tilde{u}_{pa}\tilde{u}_{ma}\tilde{u}_c+3\nu_{cc}\tilde{u}_{pc}\tilde{u}_{mc}\tilde{u}_c \end{pmatrix}. \tag{40}$$

Here we have made use of the fact that we are interested in the case where $a=b$ (and so $a\neq c$).

Considering the unforced system $\ddot{\mathbf{u}}+\Lambda\mathbf{u}+\mathbf{N}_u(\mathbf{u})=0$, the $S2$ (i.e. ath out-of-plane-only response) and $S4^{\pm}$ (i.e. ath in-plane and ath out-of-plane phase-locked response) now have the additional condition that $\tilde{U}_c=0$. However, if the cth mode exhibits a response, the backbone curves are affected due to the action of the last term in each of the first two rows of $\mathbf{N}_u$. The phase-locked, free response equations, Eqs. (15) and (16), are now

$$\left\{\omega_{na}^2-a^2\Omega^2+\frac{\nu_{aa}}{4m}\left[3U_a^2+(2+p)\tilde{U}_a^2+2\tilde{U}_c^2\right]\right\}U_a=0, \tag{41}$$

$$\left\{\tilde{\omega}_{na}^2-a^2\Omega^2+\frac{\nu_{aa}}{4m}\left[(2+p)U_a^2+3\tilde{U}_a^2+2\tilde{U}_c^2\right]\right\}\tilde{U}_a=0. \tag{42}$$

Hence the response solution is modified away from the backbone expression for $S2$ due to the presence of the $\tilde{U}_c\neq0$

response resulting in

$$U_a = 0, \quad a^2\Omega^2 = \left(\tilde{\omega}_{na}^2 + \frac{\nu_{ac}}{2m}\tilde{U}_c^2\right) + \frac{3\nu_{aa}}{4m}\tilde{U}_a^2. \tag{43}$$

Likewise, $S4^{\pm}_{a=b}$ becomes

$$a^2\Omega^2 = \left(\frac{\nu_{aa}}{2m}\left(\tilde{U}_a^2 + U_a^2\right) + \frac{\nu_{ac}}{2m}\tilde{U}_c^2\right) + \frac{1}{2}\left(\omega_{na}^2 + \tilde{\omega}_{na}^2\right), \tag{44}$$

$$\tilde{U}_a^2 = U_a^2 + \frac{2m}{\nu_{aa}}\left(\omega_{na}^2 - \tilde{\omega}_{na}^2\right). \tag{45}$$

It can be seen that the effect of the $\tilde{U}_c$ response is to shift the solutions in the frequency plane. Note that these solutions are not necessarily backbones capturing a NNM response of the system, as NNMs require a periodic motion, whereas here the frequency of the cth out-of-plane mode is unconstrained, i.e. it is not necessary that $\tilde{\omega}_{rc} = c\Omega$. However they do demonstrate that the presence of other modes makes the system appear stiffer. Physically, this can be interpreted as a change in the tension of the cable, due to the presence of other modes – the dynamic tension of a cable contains zero-frequency response terms of the form $\theta_k^2 U_k$, where θ_k is the modeshape of the kth mode [4]. Related to this, the final example in [14] shows that, when excited out-of-plane, the zero-frequency cable response in all the in-plane modes is equivalent to a correction to the static sag. It can be shown that the forced response of the ath out-of-plane mode is similarly affected, namely the cable appears stiffer.

We now consider the effect of the cth out-of-plane mode on the resonant tongue, recalling that this marks the onset of a response in the ath in-plane mode, triggered via the corresponding ath out-of-plane mode, due to phase-locking terms between these modes. Due to the additional nonlinear terms for the ath in-plane mode, due to the cth out-of-plane mode, see Eq. (40), the N_{ua}^u term, see Eq. (33), is modified to

$$N_{ua}^u = \frac{\nu_{aa}}{4m}\tilde{U}_{pa}\tilde{U}_{ma} + \frac{\nu_{ac}}{4m}\tilde{U}_{pc}\tilde{U}_{mc}. \tag{46}$$

Using Eq. (36), the stability condition, for the case where there is a constant $\tilde{U}_c$ response, may be written as

$$4\zeta_a^2\omega_{na}^2\omega_{ra}^2 + \left(\omega_{na}^2 - \omega_{ra}^2 + \frac{\nu_{aa}}{2m}\tilde{U}_a^2 + \frac{\nu_{ac}}{2m}\tilde{U}_c^2\right)^2 = \frac{\nu_{aa}^2}{16m^2}\tilde{U}_a^4. \tag{47}$$

As with the solution curves, the effect of a non-zero $\tilde{U}_c$ can be viewed as a shift in the frequency domain, equivalent to having an adjusted natural frequency, $\hat{\omega}_{na}$, of the form

$$\hat{\omega}_{na}^2 = \omega_{na}^2 + \frac{\nu_{ac}}{2m}\tilde{U}_c^2. \tag{48}$$

This adjustment to the effective linear natural frequency is identical to the adjustment for the solution curves.

Considering the cable system used in the previous figures, we can view the effect of the cth out-of-plane mode. Firstly we explore the somewhat artificial example where the forcing is such that the resonant response amplitude of the cth out-of-plane mode, $\tilde{U}_c$, is constant and the harmonics are assumed to be small. Fig. 5 considers the case where $a = b = 1$ and $c = 3$, and shows the response of the cable in terms of the resonant amplitude of the ath, i.e. first out-of-plane mode. The single-mode response to the forcing is shown, along with the bifurcation points at which the mixed-mode response is triggered (black dots) and the subsequent mixed-mode response. To aid comparison with the case where the resonant response amplitude of the third out-of-plane mode, $\tilde{U}_3$, is zero, the backbone curves and resonant tongue for the $\tilde{U}_3 = 0$ case, Fig. 4

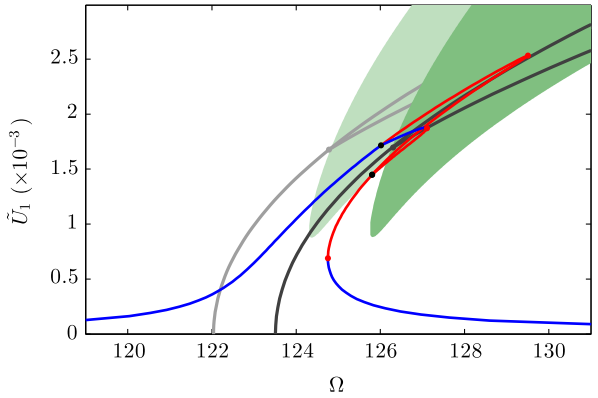

Fig. 5. Forced response of the cable using a three-mode model consisting of the first in-plane mode, the first and third out-of-plane modes, for the artificial case where the resonant response amplitude of the third out-of-plane mode, $\tilde{U}_3$, is constant, at $\tilde{U}_3 = 0.5$ mm. These responses have been computed using the following parameter values: $m = 0.04418$ kg, $\omega_{n1} = 122.04$ rad s^{-1}, $\tilde{\omega}_{n1} = 123.9$ rad s^{-1}, $\nu_{11} = 1.417 \times 10^7$ kg m^{-2} s^{-2}, $\gamma_{11} = 1.188 \times 10^4$ kg m^{-1} s^{-2}, $\gamma_{31} = 1.069 \times 10^5$ kg m^{-1} s^{-2}, $\zeta_1 = \tilde{\zeta}_1 = 0.002$ and $V = 0.015$ mm.

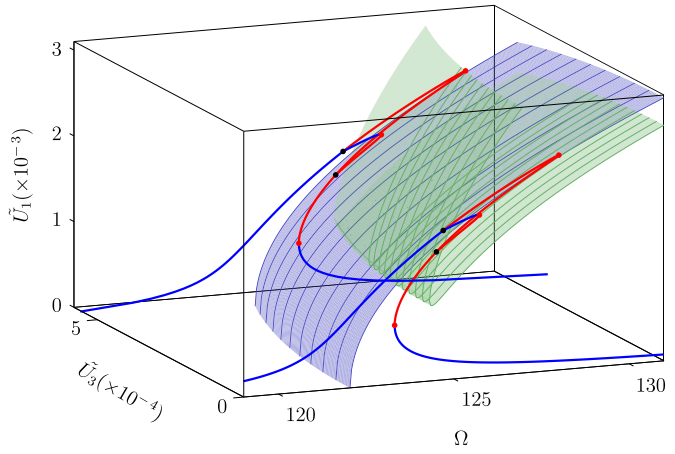

Fig. 6. Forced response of the cable using a three-mode model consisting of the first in-plane mode, the first and third out-of-plane modes, showing the plane of unforced undamped responses and the resonant tongue. This represents the artificial case where the resonant response amplitude of the third out-of-plane mode, $\tilde{U}_3$, is constant. These responses have been computed using the same parameters as those used in Fig. 5; i.e. $m = 0.04418$ kg, $\omega_{n1} = 122.04$ rad s^{-1}, $\tilde{\omega}_{n1} = 123.9$ rad s^{-1}, $\nu_{11} = 1.417 \times 10^7$ kg m^{-2} s^{-2}, $\gamma_{11} = 1.188 \times 10^4$ kg m^{-1} s^{-2}, $\gamma_{31} = 1.069 \times 10^5$ kg m^{-1} s^{-2}, $\zeta_1 = \tilde{\zeta}_1 = 0.002$ and $V = 0.015$ mm. (For interpretation of the references to colour in this figure caption, the reader is referred to the web version of this paper.)

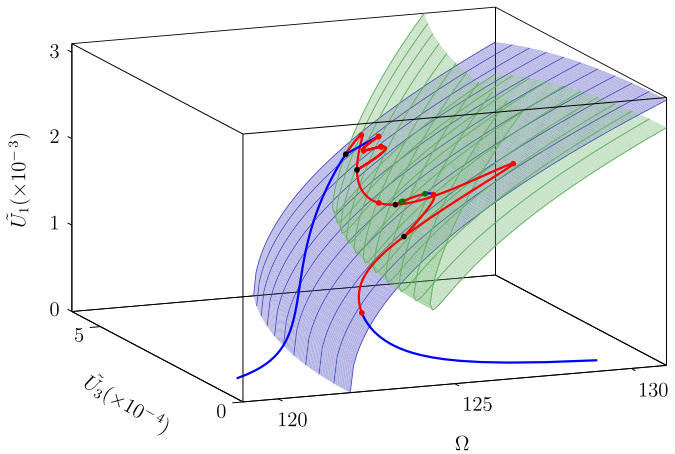

Fig. 7. Forced response of the cable using a three-mode model consisting of the first in-plane mode, and the first and third out-of-plane modes, for the case where the excitation amplitude of the forcing near the third out-of-plane mode, V_3, is constant. Blue curves denote stable solutions and red curves, unstable solutions. Black dots indicate the intersection with the resonant tongue, and the bifurcations onto the internally resonant responses. The parameters used here are identical to those used in Figs. 5 and 6; i.e. $m = 0.04418$ kg, $\omega_{n1} = 122.04$ rad s^{-1}, $\tilde{\omega}_{n1} = 123.9$ rad s^{-1}, $\nu_{11} = 1.417 \times 10^7$ kg m^{-2} s^{-2}, $\gamma_{11} = 1.188 \times 10^4$ kg m^{-1} s^{-2}, $\gamma_{31} = 1.069 \times 10^5$ kg m^{-1} s^{-2} and $\zeta_1 = \tilde{\zeta}_1 = 0.002$. Additionally, the excitation amplitudes $V_1 = 0.015$ mm and $V_3 = 0.01$ mm are used – as described in Eqs. (39). See Fig. 8 for projections from this plot onto the $\tilde{U}_1$ vs Ω, and $\tilde{U}_3$ vs Ω planes. (For interpretation of the references to colour in this figure caption, the reader is referred to the web version of this paper.)

(a), are shown in light grey and green respectively. It can be seen that the resonant tongue and unforced-undamped responses are both shifted in frequency due to the presence of the third out-of-plane mode. Likewise, the forced response is shifted, but here we note that the peak amplitude of the response is also affected due to the increased frequency at which the peak response occurs (this can be seen when compared with Fig. 4(a)).

These responses can be represented on a 3D plot, see Fig. 6. Here the backbone curve (where $\tilde{U}_3 = 0$) has been projected onto the unforced, undamped system response surface (shaded in blue) and the resonant tongue onto a resonant tongue surface (shaded in green). The two forced responses (corresponding to Figs. 4(a) and 5) are also shown for the case where there is no in-plane response, and where black dots indicate the points at which the in-plane response is triggered.

Now, considering the more realistic case in which the third out-of-plane mode is excited at a constant amplitude of support motion, due to the interactions between the two out-of-plane modes the stiffening effect varies with excitation frequency. Fig. 7 shows the response for the case where the in-plane resonant motion is zero, along with the internally resonant branches. It can be seen that the resonant tongue, which shifts as $\tilde{U}_3$ increases, due to the stiffening effect, captures these trigger points well.

This discussion indicates that, when multiple out-of-plane modes are present, while the in-plane mode is only triggered by the corresponding out-of-plane mode, i.e. when $a = b$, the presence of other out-of-plane modes will alter the behaviour

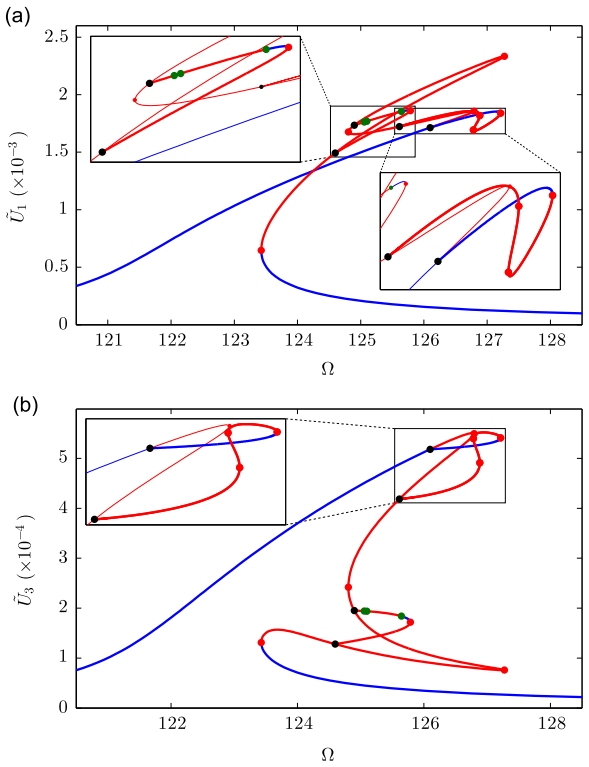

Fig. 8. Two projections from Fig. 7, showing the forced response of the cable using a three-mode model consisting of the first in-plane mode, the first and third out-of-plane modes, for the case where V_3 is constant. (a) shows $\tilde{U}_1$ vs Ω, and (b) shows $\tilde{U}_3$ vs Ω. Blue curves denote stable periodic solutions and red curves, unstable periodic solutions. Black dots indicate the intersection with the resonant tongue surface (not shown), and the bifurcations onto the internally resonant responses. The boxes show the internally resonant regions in detail. As in Fig. 7, the parameters used here are: $m = 0.04418$ kg, $\omega_{n1} = 122.04$ rad s^{-1}, $\tilde{\omega}_{n1} = 123.9$ rad s^{-1}, $\nu_{11} = 1.417 \times 10^7$ kg m^{-2} s^{-2}, $\gamma_{11} = 1.188 \times 10^4$ kg m^{-1} s^{-2}, $\gamma_{31} = 1.069 \times 10^5$ kg m^{-1} s^{-2}, $\zeta_1 = \tilde{\zeta}_1 = 0.002$, $V_1 = 0.015$ mm and $V_3 = 0.01$ mm. (For interpretation of the references to colour in this figure caption, the reader is referred to the web version of this paper.)

of this interaction. Therefore, these non-resonant out-of-plane modes must be considered in order to accurately predict the dynamic behaviour, and the points at which an internal resonance is triggered.

6. Conclusions

In this paper, the phenomenon of phase-locking between modes, and its influence on internal resonance has been considered in detail. In particular, using the example of a taut cable, expressions for both phase-locked and phase-unlocked backbone curves were developed. This analysis was initially based on two modes – one in-plane and one out-of-plane. From this it was shown that phase-locking may only occur between corresponding modes, i.e. the ath in-plane and ath out-of-plane, while two non-corresponding modes do not exhibit phase-locking. Both the phase-locked and the phase-unlocked cases lead to mixed-mode backbone curves that bifurcate from single-mode backbone curves. However, these mixed-mode backbone curves are distinct as, notably, no specific phase-condition between the linear modes is present for the phase-unlocked case.

Taking a general, two-mode, weakly nonlinear system, a stability analysis was used to show that phase-locking is necessary for an internal resonance to occur. Considering the out-of-plane forced responses of the cable, it was shown that the mixed-mode, phase-locked backbone curves correspond to internally resonant interactions, whereas the phase-unlocked backbone curves do not. This stability analysis was also applied to the cable system to demonstrate that the resonant tongue, described using the analysis, could accurately predict the onset of internal resonance.

As phase-unlocked interactions do not lead to internal resonance, it might, at first, appear that they are of little interest in the analysis of nonlinear behaviours. However, in the final section of this paper, it was demonstrated that the presence of phase-unlocked modes may lead to *stiffening* effects in the system. These were shown to influence the internally resonant responses observed between other, phase-locked, modes. This was demonstrated by extending the two-mode model of the cable, where corresponding in- and out-of-plane modes exhibit phase-locked responses, to include a third, phase-unlocked, out-of-plane mode. The stiffening effect of this third, phase-unlocked mode was shown to cause an apparent shift in the response frequency of the interactions between the other modes.

For the somewhat artificial case where the fundamental response of the third mode was held at a constant amplitude, this frequency shift was demonstrated to be constant. The more realistic case, where the response of the third mode varies under forcing, was then shown to exhibit more complex behaviours. However, these behaviours were accurately predicted by the analytical descriptions of the unforced, undamped equivalent responses, and the onset of internal resonance was predicted using the resonant tongues. This demonstrated that, while the phase-unlocked modes do not lead to internal resonance, they can alter the nature of the internal resonance between phase-locked modes.

Acknowledgements

The authors would like to acknowledge the support from the Engineering and Physical Sciences Research Council. S.A.N. and T.L.H. are supported by EP/K005375/1 and D.J.W. is supported by EP/K003836/1.

The data presented in this work are openly available from the University of Bristol repository at http://dx.doi.org/10.5523/bris.1veiinwd99sbw1rko1sp034qv4.

Appendix A. Normal form transformation

In this work we use the second order normal form technique, originally developed by [5], to apply a nonlinear transform to Eq. (1) that removes harmonic terms leaving just the resonant terms – written $\mathbf{h}$ and $\mathbf{u}$ respectively. Note that *second order* refers to the order of the differential equations, in this normal form approach the usual transformation to state-space coordinates (see for example [21,19]) is avoided, instead the transforms are applied directly to the oscillator equations resulting in more compact expressions [15,4]. Considering the transformation of the modal equation of motion to the resonant equation of motion, Eq. (3), with the restrictions that the damping is modal and the forcing in any mode is near-resonant. The derivation to find $\mathbf{N}_u$ and $\mathbf{h}(\mathbf{u})$ involves Taylor series expansions allowing the degree of accuracy (and resulting complexity) to be selected. Discussions on accuracy are given in [5,20]. Adopting the first degree of accuracy gives the approximation $\mathbf{N}(\mathbf{u}+\mathbf{h}(\mathbf{u}))\approx\mathbf{N}(\mathbf{u})=\mathbf{N}(\mathbf{u}_p,\mathbf{u}_m)$ where the transformed coordinates have been split using $\mathbf{u}=\mathbf{u}_p+\mathbf{u}_m$, resulting in a trial solution of the form given in Eq. (2). By writing $\mathbf{N}(\mathbf{u}_p,\mathbf{u}_m)=\mathbf{n}^*\mathbf{u}^*$ allows $\mathbf{N}$ to be separated into the vector $\mathbf{u}^*$, which is of length L and contains all the combinations of u_{pi} and u_{mi}, and the matrix $\mathbf{n}^*$, containing the corresponding coefficients. The transform and transformed nonlinear terms may then be written as $\mathbf{h}(\mathbf{u}_p,\mathbf{u}_m)\approx\mathbf{h}^*\mathbf{u}^*$ and $\mathbf{N}_u(\mathbf{u}_p,\mathbf{u}_m)\approx\mathbf{n}_u^*\mathbf{u}^*$, where the approximations indicate that higher-order Taylor series terms have been neglected. For the ith mode (of N) and the ℓth element in $\mathbf{u}^*$ the relationship between $\mathbf{n}^*$, $\mathbf{h}^*$ and $\mathbf{n}_u^*$ is given by

$$n_{i,\ell}^*=n_{u,i,\ell}^*+\beta_{i,\ell}^*h_{i,\ell}^* \quad \text{with: } \beta_{i,\ell}^*=\left(\sum_{n=1}^{N}\left\{(s_{pn\ell}-s_{mn\ell})\omega_{rn}\right\}\right)^2-\omega_{ri}^2, \tag{A.1}$$

where $s_\bullet$ is defined via the general form for the ℓth element in $\mathbf{u}^*$,

$$u_\ell^*=\prod_{n=1}^{N}\left(u_{pn}^{s_{pn\ell}}u_{mn}^{s_{mn\ell}}\right). \tag{A.2}$$

When $\beta_{i,\ell}^*=0$, the term is resonant and we set $n_{i,\ell}^*=n_{u,i,\ell}^*$, otherwise the term is placed in the transform using $h_{i,\ell}^*=n_{i,\ell}^*/\beta_{i,\ell}^*$. Note that we generate matrix $\boldsymbol{\beta}^*$ with the $[i,\ell]$th element being $\beta_{i,\ell}^*$ however this cannot be used in matrix multiplications as the relationship with $\mathbf{n}^*$ is indicial. See, for example, [5,15,4] for a derivation of the expressions presented above. These references also deal with the case where the forcing is non-resonant and the damping is not necessarily resonant.

References

[1] J. Guckenheimer, P. Holmes, *Nonlinear Oscillations, Dynamical Systems, and Bifurcations of Vector Fields*, Springer-Verlag, New York, 1983.
[2] M. Cartmell, *Introduction to Linear, Parametric and Nonlinear Vibrations*, Chapman and Hall, London, UK, 1990.
[3] A. Nayfeh, P. Pai, *Linear and Nonlinear Structural Mechanics*, Wiley, Weinheim, Germany, 2004.
[4] D.J. Wagg, S.A. Neild, *Nonlinear Vibration with Control*, second edition, Springer-Verlag, Berlin, Germany, 2014.
[5] S.A. Neild, D.J. Wagg, Applying the method of normal forms to second-order nonlinear vibration problems, *Proceedings of the Royal Society, Part A: Mathematical, Physical and Engineering Science* 467(28) (2011) 1141–1163.
[6] A.F. Vakakis, L.I. Manevitch, Y.V. Mikhlin, V.N. Pilipchuk, A.A. Zevin, *Normal Modes and Localization in Nonlinear Systems*, Wiley, New York, 1996.
[7] A.F. Vakakis, R.H. Rand, Normal modes and global dynamics of a two-degree-of-freedom non-linear system – I. Low energy, *International Journal of Non-linear Mechanics* 27 (5) (1992) 861–874.
[8] G. Kerschen, M. Peeters, J.C. Golinval, A.F. Vakakis, Nonlinear normal modes, Part I: *a useful framework for the structural dynamicist*, *Mechanical Systems and Signal Processing* 23 (Sp. Iss. (SI) 1) (2009) 170–194.
[9] R. Lewandowski, Solutions with bifurcation points for free vibration of beams: *an analytical approach*, *Journal of Sound and Vibration* 177 (1994) 239–249.
[10] R. Lewandowski, On beams, membranes and plates backbone curves in a cases of internal resonance, *Meccanica* 31 (1996) 323–346.
[11] A. Cammarano, T.L. Hill, S.A. Neild, D.J. Wagg, Bifurcations of backbone curves for systems of coupled nonlinear oscillators, *Nonlinear Dynamics* 77 (1–2) (2014) 311–320.

[12] T.L. Hill, A. Cammarano, S.A. Neild, D.J. Wagg, Out-of-unison resonance in weakly-nonlinear coupled oscillators, *Proceedings of the Royal society, Part A: Mathematical, Physical and Engineering Science* 471 (2015) paper 20140332.
[13] T.L. Hill, A. Cammarano, S.A. Neild, D.J. Wagg, Interpreting the forced responses of a two-degree-of-freedom nonlinear oscillator using backbone curves, *Journal of Sound and Vibration* 349 (2015) 276–288.
[14] S.A. Neild, A.R. Champneys, D.J. Wagg, T.L. Hill, A. Cammarano, The use of normal forms for nonlinear dynamical systems, *Philosophical Transactions of the Royal Society, Part A: Mathematical, Physical and Engineering Science* 373 (2015). paper 20140404.
[15] S.A. Neild, Approximate methods for analysing nonlinear structures, in: L.N. Virgin, D.J. Wagg (Eds.) *Exploiting Nonlinear Behaviour in Structural Dynamics*, Springer-Verlag, Berlin, Germany, 2012.
[16] P. Warnitchai, Y. Fujino, T. Susumpow, A non-linear dynamic model for cables and its application to a cable-structure system, *Journal of Sound and Vibration* 187 (1995) 695–712.
[17] A. Gonzalez-Buelga, S.A. Neild, D.J. Wagg, J.H.G. Macdonald, Modal stability of inclined cables subjected to vertical support excitation, *Journal of Sound and Vibration* 318 (3) (2008) 565–579.
[18] J.H.G. Macdonald, M.S. Dietz, S.A. Neild, A. Gonzalez-Buelga, A.J. Crewe, D.J. Wagg, Generalised modal stability of inclined cables subjected to support excitations, *Journal of Sound and Vibration* 329 (21) (2010) 4515–4533.
[19] A.H. Nayfeh, *Method of Normal Forms*, Wiley, Weinheim, Germany, 1993.
[20] S.A. Neild, D.J. Wagg, A generalized frequency detuning method for multidegree-of-freedom oscillators with nonlinear stiffness, *Nonlinear Dynamics* 73 (2013) 649–663.
[21] L. Jezequel, C.-H. Lamarque, Analysis of non-linear dynamic systems by the normal form theory, *Journal of Sound and Vibration* 149 (3) (1991) 429–459.